

# Two voltage-current load signature classes for residential consumers

Dadiana-Valeria Căiman  
Automation and Applied Informatics  
Politehnica University Timisoara  
Timisoara, Romania  
e-mail [dadiana.grando@aut.upt.ro](mailto:dadiana.grando@aut.upt.ro)

Toma-Leonida Dragomir  
Automation and Applied Informatics  
Politehnica University Timisoara  
Timisoara, Romania  
e-mail [toma.dragomir@upt.ro](mailto:toma.dragomir@upt.ro)

**Abstract**— Load current signatures are commonly used to characterize household electricity consumers. This paper introduces a new load signature class, the ellipse class, in addition to the tangent class already used in [10]. For both classes the signature consists of the set of parameters assigned to the two types of analytical functions. Signature determination is based on the operation of samples obtained at a very low frequency of approximately 20 Hz. This paper illustrates applications to both a single consumer and two consumers of the same class or of different classes.

**Keywords**—load monitoring, load signature, voltage-current trajectory, genetic algorithms, smart meter

## I. INTRODUCTION

Voltage-current load signatures (VILS) of consumers and voltage-current trajectories (VIT) constitute evaluation tools for consumers for several reasons, mainly due to their reactive features. Concerns related to signatures led to numerous approaches to address them reported in the literature.

In [1], H. Y. Lam introduces the taxonomy that addresses the VIT. In order to translate the voltage-electric current curve into a signature, the geometry of the curve is analysed. This geometry is described by 8 parameters: “asymmetry, looping direction, curvature of mean line, self-intersection, slope of middle segment, area of left and right segments, peak of middle segment.” In [2], T. Hassan adds some more parameters to the 8 suggested by Lam.

In [3], VIT are used in their initial form in order to train a neural network. The data needed was acquired at minimum 4 kHz sampling frequency so that the identification of the home appliance to be successful. In [4], the consumer is identified through a hybrid method that includes the curve geometry (VIT) and the information related to harmonics, active power and reactive power. In [5], the VIT is deconstructed into the active voltage-current curve that is used in the identification, and the non-active voltage-current curve, using Fryze theory.

In [6], the influence of the input voltage variation on the VIT is studied. The results of the study show that voltage variations do not affect the size and the form of the trajectory, but they affect the signature, that is the 8 parameters which describe the geometry of the curve.

In [7] and [8], the VIT translated through a pixel matrix is used as a starting point. Methods of image recognition are considered for identification: convolutional neural network in

[7] and elliptical Fourier descriptors as the basis for a neural network in [8]. Both papers use the PLAID data base acquired at a sampling rate of 30 kHz. In [7] the WHITED data base is also used (data acquired at 44 kHz).

In [9], a classification of consumers is presented in accordance with the parameters used to achieve the load signatures. Among these parameters VIT is mentioned.

Paper [10] presents a method of associating analytical load signatures of VIT type based on the trigonometric function tangent. The parameterization of the signatures is achieved by using genetic algorithms (GA). The analytical expression defines the class and the parameters set represents the signature. This article extends the approach in paper [10] by taking into account a new class of signatures, of elliptic type, and by presenting the modality for identifying the two classes of signatures in the event of registering a cumulated consumption from consumers belonging to both classes.

Section II of the paper discusses the measurement scheme and the studied signature classes. Section III presents the analysed cases and section IV presents the results. The final section concludes the paper.

## II. MEASUREMENT CONDITIONS. SIGNATURES

### A. Measurement scheme

The measurement scheme used in order to determine the signatures is reflected in Fig. 1. This scheme uses the STM board [11], under the same conditions as the paper [10]. The software associated to the evaluation board allows acquiring momentary values of the voltage, the total current absorbed by the consumers connected to the power unit, the consumed reactive power etc. in sets corresponding to 1024 moments. The data is obtained at a sampling time of around 2.5 periods of voltage supply (approximately 20 Hz).

Further we will refer to *single consumer* when there is just one consumer in the circuit and *multiple consumer* when there are 2 or more consumers connected in-line.

### B. Voltage-current signatures

VILS are determined from the matching values  $(v_k, i_k)$  obtained with the help of the circuit in Fig. 1 at instants  $t_k$ ,  $k=1, 2, \dots, k_{\max}$ . We mark with  $M$  the set of measured points  $M=\{(v_k, i_k)\}$ . The VILS of a consumer, referred to as  $S$ , represents an analytical function  $S: D_v \rightarrow D_i$ , where  $D_v$  represents the domain of voltage values  $v(t)$  supplied by the

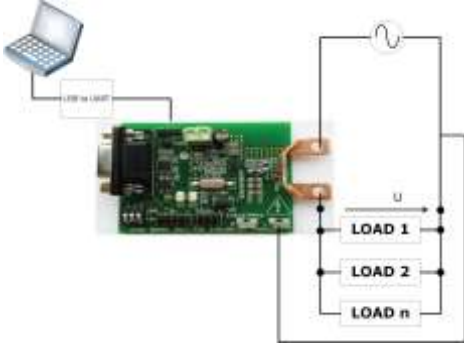


Fig. 1. Measurement scheme

network, and  $D_i$  the domain of absorbed current values  $i(t)$ . The expression of the function  $S$  allows the division of consumers in classes of load signatures. Hereinafter, only two classes are taken into account: s-tangent class, referred to as  $C_{tg}$ , and s-ellipsis class, referred to as  $C_{ell}$ .

The class  $C_{tg}$ , defined in (1), was introduced in paper [10]:

$$S_{tg}(v) : \underbrace{\left(-c_l \frac{\pi}{2} - d_l, c_r \frac{\pi}{2} - d_r\right)}_{D_v} \rightarrow \infty$$

$$S_{tg}(v) = K_{tg}(v) \cdot \left\{ \left[ a_l tg \frac{v+d_l}{c_l} - a_r tg \frac{v_b+d_l}{c_l} + a_r tg \frac{v_b+d_r}{c_r} \right] \cdot \frac{1 - \text{sgn}(v - v_b)}{2} + b + \left[ a_r tg \frac{v+d_r}{c_r} \right] \cdot \frac{1 + \text{sgn}(v - v_b)}{2} \right\} \quad (1)$$

In (1):  $a_l, b_l, c_l, d_l, a_r, b_r, c_r, d_r, v_b$  are real parameters,  $c_l > 0$ ,  $c_r > 0$ ,  $v_b$  takes a value in  $D_v$ , the indexes „l” and „r” are used with the meaning of „left” and „right”,  $\text{sgn}(v)$  is the signum function, and

$$K_{tg}(v) = \begin{cases} 1, & \text{if } v \in \left[-\frac{\pi}{2} c_l - d_l + \varepsilon, \frac{\pi}{2} c_r - d_r - \varepsilon\right] \\ 0, & \text{else} \end{cases} \quad (2)$$

Here  $\varepsilon > 0$  ensures avoiding the asymptotic values of the tangent function.

To obtain  $S_{tg}(v)$  the parameters from (1) are determined based on set  $M$ . These parameters are part of sets (3a) and (3b) for the ascending and descending branch of signature  $S_{tg}(v)$ :

$$p_{consumer1-a} = \{a_l^a, b^a, c_l^a, d_l^a, a_r^a, c_r^a, d_r^a\} \quad (3a)$$

$$p_{consumer1-d} = \{a_l^d, b^d, c_l^d, d_l^d, a_r^d, c_r^d, d_r^d\} \quad (3b)$$

To the VILS  $C_{ell}$  introduced in this paper corresponds to the rotated ellipse (4). In (4):  $a, b, \beta, A$ , are real parameters,  $V_{\max} = -V_{\min} > 0$ .  $K_{ell}$  is obtained through (5).

$$S_{ell}(v) : \underbrace{\{v_k | \Delta(v) \geq 0\}}_{D_v} \rightarrow \infty, \Delta(v) = \left(1 - \frac{v^2}{a^2}\right) - \left(1 - \frac{b^2}{a^2}\right) \sin^2 \beta,$$

$$S_{ell,1,2}(v) = K_{el}(v) \cdot \frac{\left[\left(1 - \frac{b^2}{a^2}\right) \sin^2 \beta\right] \cdot \text{xtg}(v) \mp b \sqrt{\Delta(v)}}{1 - \left(1 - \frac{b^2}{a^2}\right) \sin^2 \beta} \quad (4)$$

$$\cdot \left(1 + A \sin \left(3\pi \frac{v - v_{\min}}{v_{\max} - v_{\min}}\right)\right) \cdot e^{\frac{|v|}{c_{\max}}}$$

$$K_{ell}(v) = \begin{cases} 1, & \text{if } \Delta(v) \geq 0 \\ 0, & \text{else} \end{cases} \quad (5)$$

And this time, the determination of the signature  $S_{ell}(v)$  means the determination of all the parameters in (4) based on set  $M$ . In this particular case the parameters are aggregated in:

$$p_{consumer2} = \{a, b, \beta, A, k\}. \quad (6)$$

Fig. 2 exemplifies the two types of signatures. “a” and “d” highlight the ascending and descending branches of the signatures.

### III. THE STUDIED CASES OF GENETICAL ALGORITHMS

In the sequel we focus on obtaining the VILS in 4 different situations: Case-1 – two single consumers and  $k_{\max} = 1024$ , Case-2 and Case-3 – one multiple consumer consisting of two single consumers in different operating conditions and respectively the same operating conditions,  $k_{\max} = 3 \times 1024$ , Case-4 – one multiple consumer, just like in case 3, and  $k_{\max} = 1024$ . The signatures are determined using genetic algorithms.

Case 1 refers to the VILS of a laptop from  $C_{tg}$  class (Case-1.1) and of a refrigerator from  $C_{ell}$  class (Case-1.2), from separate sets of measurements (each with 1024 pairs  $(v_k, i_k)$ ). For the GA the configuration of an individual corresponds to  $p_{consumer1-a}$  set for the ascending line of the signature and to  $p_{consumer1-d}$  set for the descending line of the signature. The fitness function is described by the (7) with  $i(v_k) = S_{tg}(v_k)$ :

$$F_{fitness} = \frac{1}{N} \sum_k |i_k - i(v_k)| \cdot \left(1 + 0.2 e^{\frac{-v_k}{V^*}}\right) \quad (7)$$

Parameter  $V^*$  is chosen so that the points situated in the central area of the domain  $D_v$  have a non-negligible weight in the fitness expression.

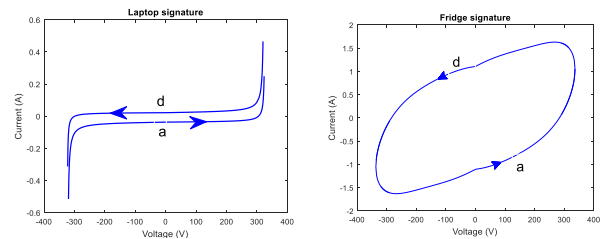


Fig. 2. Signatures: tangent class, elliptic class

In Case-1.2 the configuration of an individual corresponds to  $p_{\text{consumer2}}$  set and to the fitness function (7) with  $i(v_k) = S_{\text{ell}}(v_k)$ .

In Case 2 the multiple consumer is composed of 2 single consumers: consumer 1 – a laptop that functions in continuous mode and belongs to the  $C_{\text{tg}}$  class and consumer 2 – a refrigerator that functions in intermittent mode and belongs to the  $C_{\text{ell}}$  class. In order to expand the precision in determining the signatures, set M was formed by combining 3 sets of measurements.

Due to the intermittent running of consumer 2, the signature for consumer 1 is determined during a first stage, operating with a subset  $M_1$  of set M made of points  $(v_k, i_k)$  at instants when consumer 2 is off. The separation of set  $M_1$  from set M is achieved automatically after reordering set M according to the recorded reactive power. The set  $M_1$  contains points that have a reduced consumption of reactive power. After obtaining set  $M_1$  and its decomposition in complementary subsets  $M_{1-a}$  and  $M_{1-d}$  – corresponding to the ascending and the descending lines of the VILS, the same procedure should be followed as in Case 1 to determine the parameters, specifying that the result may be part of any of the two classes. The decomposition is achieved using the method from paper [10].

Next, in a second stage the signature for consumer 2 is determined using set  $M_{12} = M \setminus M_1$ , maintaining for consumer 1 the signature from the first stage. Subset  $M_{12}$  is decomposed in two complementary subsets,  $M_{12-a}$  and  $M_{12-d}$ , corresponding to the ascending and descending lines of the VILS. Due to the fact that both consumers have continuous running, the GA operates both on ascending and descending lines of signatures for individuals resulting from the concatenations:  $p_{\text{consumer12-a}} = p_{\text{consumer1-a}} \cup p_{\text{consumer2}}$ , and  $p_{\text{consumer12-d}} = p_{\text{consumer1-d}} \cup p_{\text{consumer2}}$ .

In both stages the fitness function takes the form (7), with  $i(v_k) = S_{\text{tg}}(v_k)$  in the first stage, and in the second stage with:

$$i(v_k) = S_{\text{tg}}(v_k) + S_{\text{ell}}(v_k) \quad (8)$$

In Case 3 the multiple consumer has the same composition as in Case 2, but the running mode is continuous. Set M integrates 3 sets of measurements. Using the allocation algorithm mentioned, this set is divided into 2 complementary subsets,  $M_a$  and  $M_d$ , associated to the ascending and descending lines of the signatures. The parameters are thus aggregated for individuals with the form:  $p_{\text{consumer-a}} = p_{\text{consumer1-a}} \cup p_{\text{consumer2}}$  and  $p_{\text{consumer-d}} = p_{\text{consumer1-d}} \cup p_{\text{consumer2}}$ . The fitness function takes the form (7) with  $i(v_k)$  calculated with (8).

Case 4 resumes Case 2 and Case 3 given that set M is formed from only one set of measurements. The purpose of this case is to find out how the number of measurement sets influences the determined signatures.

#### IV. EXPERIMENTAL RESULTS

##### A. Voltage-current load signature for single consumers in CASE 1

Fig. 3 shows intermediate and final results obtained in Case 1.1. Fig. 3-a) illustrates the selected points of set M used for determining the signature after the allocation algorithm [10] has been applied: the points associated with the descending line are marked with red, whilst blue designates the points associated with the ascending line. Fig. 3-b) pictures the graphics signature associated to the laptop. The connection between the signature constitutive lines and the points in the first picture is shown in Fig. 3-c) and 3-d). Fig. 4 presents similar results for the Case-1.2.

The values of the parameters (3a) and (3b) of the laptop signature  $S_{\text{tg}}(v)$  – Case-1.1 – are those in TABLE 1, second column. The fitness functions for the ascending and descending lines are close: 0.04525, and 0.04211.

The fourth column of the same table illustrates the values of the 5 parameters of the function  $S_{\text{ell},2}(v)$ . In Case-1.2 the

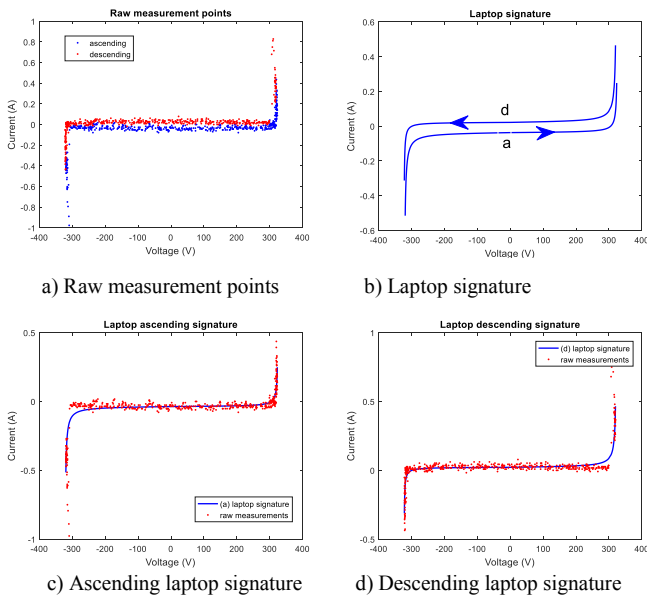


Fig. 3. Results for Case-1.1

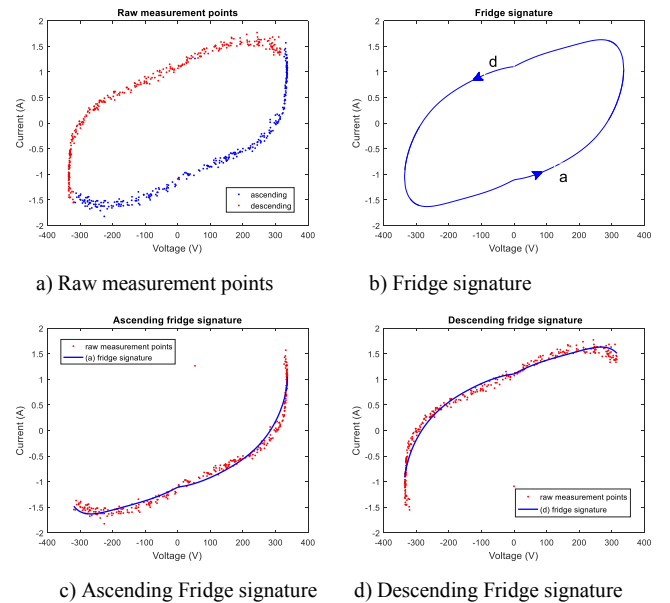


Fig. 4. Results for Case-1.2

result was a fitness function of 0.13627, a bit above the double of the previous case, while the number of generations was 289.

TABLE 1

Case 1.1 Laptop		Case 1.2 Fridge	
(a) GA Iterations	288	(a) GA Iterations	289
(a) Size of Generation	200	(a) Size of Generation	200
(a) Fitness	0.04525	(a) Fitness	0.13627
$a_l^a$	133.78531 [100, 350]	$a$	336.57001 [290, 450]
$b^a$	0.03687/[-0.2, 0.2]	$b$	1.06762/[0.001, 2]
$c_l^a$	216.94754 [210, 400]	$\beta$	0.00202 [0.0001, 0.05]
$d_l^a$	-17.45870/[-25, 0]	$A$	-0.03537/[-0.3, 0.3]
$a_r^a$	266.24200/[100, 270]	$c$	2.95567/[1, 10]
$c_r^a$	209.23763/[205, 230]		
$d_r^a$	2.33883/[-15, 10]		
(d) GA Iterations	404	(d) GA Iterations	51
(d) Size of Generation	200	(d) Size of Generation	200
(d) Fitness	0.04211	(d) Fitness	0.157690
$a_l^d$	393.92474/[100, 450]	$a$	336.57001
$b^d$	-0.02176/[-0.2, 0.2]	$b$	1.06762
$c_l^d$	216.45137/[210, 400]	$\beta$	0.00202
$d_l^d$	-15.79122/[-27, 0]	$A$	-0.03537
$a_r^d$	134.340140/[100, 250]	$c$	2.95567
$c_r^d$	208.632562/[205, 230]		
$d_r^d$	4.32034197/[-15, 10]		

### B. Obtained patterns on pairs of defferent power consumers

a) The starting experimental data in Case 2 are illustrated in Fig. 5, and the results are presented in Fig. 6.

Fig. 5-a) illustrates the sets of points  $M_{1-a}$  and  $M_{1-d}$ . They belong to consumer 1 for the timespans in which consumer 2 is shutting-down automatically. Fig. 5-b) depicts the sets of points  $M_{12-a}$ ,  $M_{12-d}$  that result after applying the allocation algorithm to set  $M_{12}$ .

In Fig. 6-a) and 6-b) the ascending and descending lines of the consumer 1 signature are highlighted in blue. This consumer is functioning in continuous mode. The signature is obtained while consumer 2 is off. The signature is related to

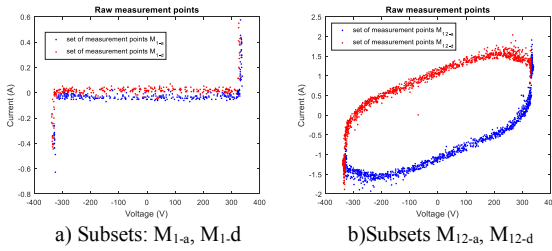


Fig. 5. Subset of sets  $M_1$  and  $M_{12}$

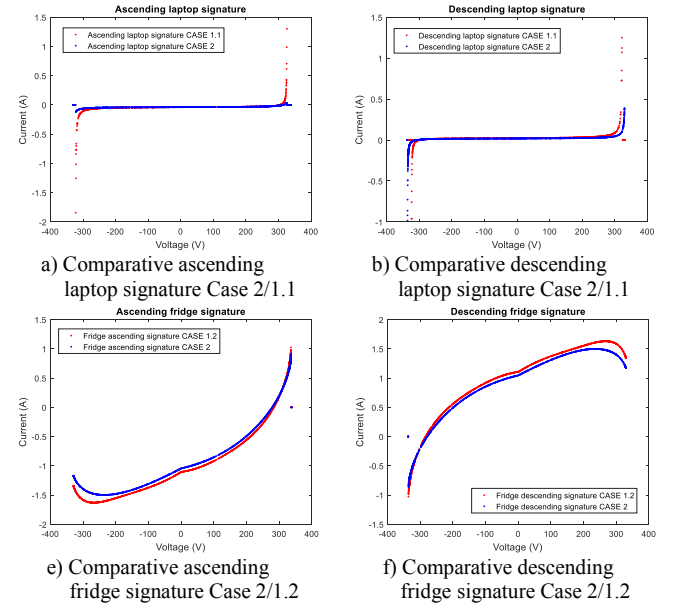


Fig 6. Comparative results Case-2/Case-1.1 & Case-1.2

the signature resulted in Case-1.1 in the graph representation and is highlighted in red.

Fig. 6-c) and 6-d) highlight in blue the ascending and descending lines of the signatures from consumer 2 which function in intermittent mode. The signature is related to the signature resulted in Case-1.2 in the graph representation.

Fig. 7 illustrates the integrated signatures of consumer 1 (a), consumer 2 (b) and the combined signature of the two consumers (c), that is the sum  $S_{lg}(v) + S_{el}(v)$ .

The first and the second columns of TABLE 2 show the associated parameters of the laptop signature,  $p_{consumer1-a}$ ,  $\cup$   $p_{consumer1-d}$ , the third and the fourth columns show the associated parameters of the refrigerator signature,  $p_{consumer2}$ , and the fifth to eighth columns show the laptop and refrigerator parameters that correspond to the combined signature  $p_{consumer12-a} = p_{consumer1-a} \cup p_{consumer2}$  și  $p_{consumer12-d} =$

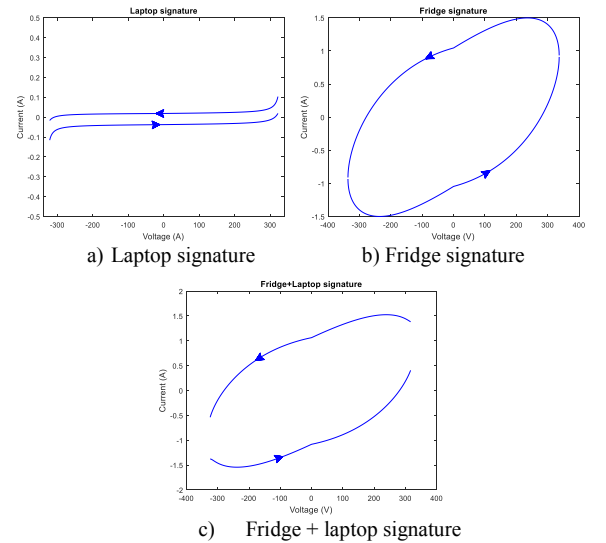
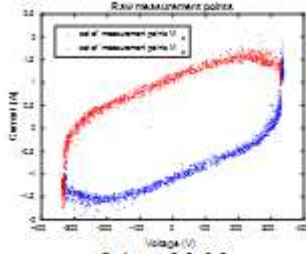


Fig.7 Signatures in CASE 2



Subsets  $M_1$ ,  $M_2$   
Fig. 8. Subsets  $M_1$  and  $M_2$

$p_{consumer1-d} \cup p_{consumer2}$ .

The differences between the fitness functions may be observed in distinctive cases.

TABLE 2

Laptop Consumer 1		Fridge Consumer 2		Fridge+Laptop CASE 2	
(a) GA Iterations 248		a	336.82273	(a) GA Iterations 145	(d) GA Iterations 51
(a) Size of Generation: 200		b	1.04721	(a) Size of Generation: 200	(d) Size of Generation: 200
(a) Fitness 0.03836		$\beta$	0.00210	(a) Fitness 0.14421	(d) Fitness 0.149503
$a_l^a$	278.80488 [100, 350]	A	0.00218	$a_l^a$	278.8048
$b^a$	0.03737 [-0.2, 0.2]	c	4.57421	$b^a$	0.03737
$c_l^a$	218.18408 [210, 400]			$c_l^a$	218.1840
$d_l^a$	-10.74709 [-25, 0]			$d_l^a$	-10.74709
$a_r^a$	227.43714 [100, 250]			$a_r^a$	227.4371
$c_r^a$	215.91227 [205, 230]			$c_r^a$	215.91227
$d_r^a$	0.42075 [-15, 10]			$d_r^a$	0.42075
(d) GA Iterations 101				a	336.8227 [290, 450]
(d) Size of Generation: 200				b	1.04721 [0.001, 2]
(d) Fitness 0.03812				$\beta$	0.00210 [0.0001, 0.05]
$a_l^d$	438.21055 [100, 450]	A	0.00218 [-0.3, 0.3]	A	0.00218
$b^d$	-0.01860 [-0.2, 0.2]	c	4.57421 [1, 5]	c	4.57421
$c_l^d$	230.72935 [210, 400]				
$d_l^d$	-25.62327 [-27, 0]				
$a_r^d$	243.18060 [100, 250]				
$c_r^d$	213.64909 [205, 230]				
$d_r^d$	3.27611 [-15, 10]				

In TABLE 1 and 2, the domains in which the GA generated values for parameters are marked between brackets. In the cases where the domains are not marked, the parameters' values are derived from former calculation phases.

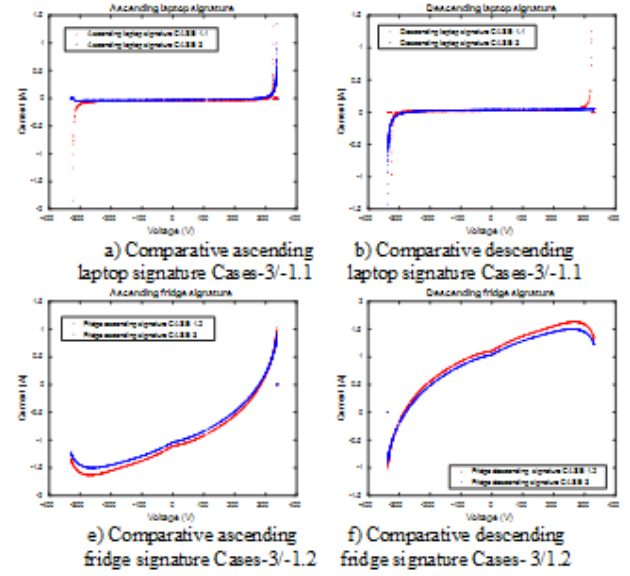


Fig. 9. Comparative results Cases-3/Case-1.1 & Case-1.2

b) For Case 3, when both consumers function in continuous mode, the results of applying the allocation algorithm are illustrated in Fig. 8: with blue highlighting the set of points  $M_a$  associated to the ascending line, and red highlighting the set of points  $M_d$  associated to the descending line.

Fig. 9 illustrates the comparative results of the signatures obtained in Case 3 for the two consumers and the individual results gathered in Case 1. In Fig. 9-a) and 9-b) the VILS of the laptop (consumer 1) are compared, while in Fig. 9-c) and 9-d) the VILS of the refrigerator (consumer 2) are compared. The signatures for the two consumers and the VILS for the cumulated consumption are illustrated in Fig. 10.

TABLE 3 lists the parameters resulted from the implementation of the GA as follows: in columns 1 and 2 the parameters associated with the laptop,  $p_{consumer1-a}$ ,  $\cup$   $p_{consumer1-d}$ , in columns 3 and 4 the parameters associated with the refrigerator,  $p_{consumer2}$ , while in columns 5 and 6 the parameters of both consumers  $p_{consumer-a} = p_{consumer1-a} \cup p_{consumer2}$  and

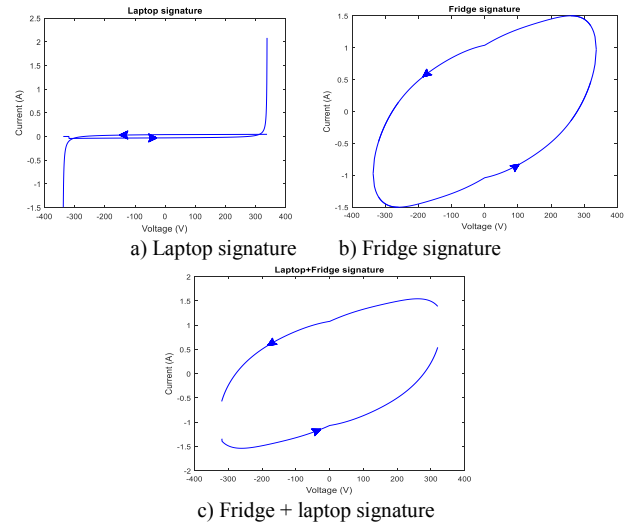
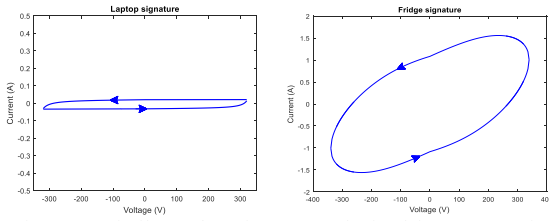
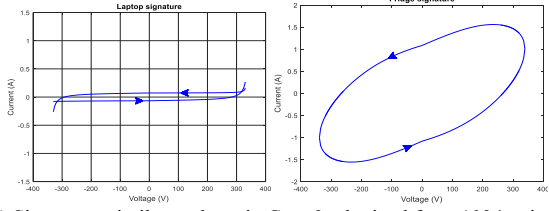


Fig. 10. Signatures in CASE 3



a) Signatures similar to those in Case 2, obtained from 1024 points



b) Signatures similar to those in Case 3, obtained from 1024 points

Fig. 11. Signatures in Case 4

$$p_{\text{consumer-d}} = p_{\text{consumer1-d}} \cup p_{\text{consumer2-d}}$$

TABLE 3

Laptop Consumer 1		Fridge Consumer 2		Fridge+Laptop CASE 3	
$a_l^a$	114.9701	a	336.6665	(a) GA Iterations 300	(d) GA Iterations 92
$b^a$	0.02936	b	1.01283	(a) Size of Generation 200	(d) Size of Generation 200
$c_l^a$	334.516	$\beta$	0.00203	(a) Fitness 0.13040	(d) Fitness 0.12548
$d_l^a$	-0.12866	A	-0.02518	$a_l^a$	$a_l^d$
$a_r^a$	106.2496	c	3.64896	$b^a$	$b^d$
$c_r^a$	209.5990			$c_l^a$	$c_l^d$
$d_r^a$	-9.69716			$d_l^a$	$d_l^d$
$a_l^d$	75.74147			$a_r^a$	$a_r^d$
$b^d$	-0.03934			$c_r^a$	$c_r^d$
$c_l^d$	217.2448			$d_r^a$	$d_r^d$
$d_l^d$	-1.37700			a	a
$a_r^d$	209.2516			b	b
$c_r^d$	385.4641			$\beta$	$\beta$
$d_r^d$	15.78247			A	A
				c	c

For Case 4, which returns to Cases 2 and 3, in the event that set M relies on one set of measurements ( $k_{\max}=1024$ ), Fig. 11-a) illustrates the counterpart signatures from Case 2 (consumer 2 – the refrigerator – functions in intermittent

mode, while consumer 1 – the laptop – in continuous mode), whereas Fig. 11-b) shows the counterpart signatures from Case 3 (both consumers run continuously). It can be observed that the results are similar to those from Case 2 and Case 3 (three sets of values).

## V. CONCLUSION

Numerous domestic consumers present voltage-current load signatures that can be divided into classes that can be further described analytically through tangent or elliptical functions. The signatures can be acquired through the method presented in the paper, based on the aggregation of the parameters signatures in specific vectors using GA. The implementation of the method is presented in case studies of two different types of consumers, having the same functioning or different type of running. One important aspect of using the method is that, contrary to other methods of signature findings, the frequency used to acquire the measured values is only 20 Hz (2.5 duration of the network voltage). For the above studied cases, sets with 1024 measurement points were sufficient.

The presented study is part of a research intended to complete the literature on analytic signatures for domestic consumers that can be used to automatically quantify the individual signatures from composite consume.

## REFERENCES

- [1] H.Y.Lam, G.S.K.Fung, and W.K.Lee, "A novel method to construct taxonomy of electrical appliances based on load signature," *IEEE Transaction on Consumer Electronics*, Vol. 53, No. 2, pp. 653-660, May 2007.
- [2] T. Hassan, F. Javed and N. Arshad, "An Empirical Investigation of V-I Trajectory based Load Signatures for Non-Intrusive Load Monitoring," *IEEE Transaction on Smart Grid* 5 (2), pp. 870-878, 2014.
- [3] K.-S. Barsim, L. Mauch, B. Yang, "Neural Network Ensembles to Real-time Identification of Plug-level Appliance Measurements," <https://arxiv.org/abs/1802.06963>, 2018.
- [4] N. Iksan, J. Sembiring, N. Haryanto, S. H. Supangkat, "Appliances identification method of non-intrusive load monitoring based on load signature of V-I trajectory," *IEEE International Conference on Information Technology Systems and Innovation (ICITSI)*, 2015.
- [5] D.F. Teshome, T.D.Huang, and K.-L. Lian, "Distinctive Load Feature Extraction based on Fryze's time-domain power theory," *IEEE Power and Energy Technology Systems Journal*, Vol. 3, No. 2, pp. 60-70, June 2016.
- [6] A. A. Kholeif, H. A. Abd el-Ghany, A. M. Azmy, "Impact of Supply Voltage Variation on V-I Trajectory Identification Method", *Nineteenth International Middle East Power Systems Conference (MEPCON)*, Menoufia University, Egypt, December 2017.
- [7] L. De Baets, J. Ruysinck, C. Develder, T. Dhaene, D. Deschrijver, "Appliance classification using VI trajectories and convolutional neural networks", *Energy and Buildings*, Vol. 158, pp. 32-36, 2018.
- [8] L. De Baets, C. Develder, T. Dhaene and D. Deschrijver, "Automated classification of appliances using elliptical Fourier descriptors", *IEEE International Conference on Smart Grid Communication*, Dresden, Germany, October 2017.
- [9] N. Sadeghianpourhamami, J. Ruysinck, D. Deschrijver, T. Dhaene, C. Develder, "Comprehensive feature selection for appliance classification in NILM", *Energy and Buildings*, Vol. 151, pp.98-106, 2017.
- [10] D.-V. Căiman, T.L. Dragomir "Non – Intrusive load monitoring: analytic expression as load signature," *12th International Symposium on SACI 2018*, pp. 15-20.
- [11] <http://www.st.com/en/data-converters/stpm32.html#sw-tools-scroll>, May 2018